5-6-2020

A Study of the Efficiency and Effectiveness of the First Four Iterations of Sierpinski carpet Fractal-like Fins at Increasing Angles in Natural Convection

Sophia N. Fleri
Georgia Southern University

A Study of the Efficiency and Effectiveness of the First Four Iterations of Sierpinski carpet Fractal-like Fins at Increasing Angles in Natural Convection

An Honors Thesis submitted in partial fulfillment of the requirements for Honors in the *Department of Mechanical Engineering*

By
Sophia Fleri

Under the mentorship of *Dr. David Calamas*

ABSTRACT

Fractal geometries have been found in several studies to increase a fin's thermal performance. Both the reductions of volume and mass accompanied by an increase in performance are desirable to prevent malfunction of the device through passive heat dissipation. The Sierpinski carpet fractal pattern, beginning with a basic square geometry in which an increasing number of perforations are incorporated through each successive iteration, reduces the fin's mass while increasing its surface area simultaneously; this increase in surface area increases the rate of heat transfer experienced across the fin. The first four iterations of the Sierpinski carpet pattern, each with identical dimensions and material, were compared at orientations of 0°, 45°, or 90° to determine which iteration yielded the greatest efficiency, effectiveness, and effectiveness per unit mass. This experiment was performed in a natural convection environment with constant heat flux of 20 Watts applied at the base of the fin. It was found that across all iterations, an orientation of 90° yielded the highest efficiency, effectiveness, and effectiveness per unit mass with two negligible exceptions for the effectiveness and effectiveness per unit mass of the 1st iteration at 0°.

Thesis Mentor:________________________

Dr. David Calamas

Honors Director:_______________________

Dr. Steven Engel

April 2020
Department of Mechanical Engineering
University Honors Program
Georgia Southern University

ACKNOWLEDGMENTS

I would like to express endless gratitude to my faculty advisor, Dr. David Calamas, for his guidance, patience, and his ability to simplify complex concepts, as well as his essential role in providing the means of experimentation and calculation. Additionally, I would like to thank graduate student, Haidar Khalil, who helped in the completion of all the trials and records even at odd hours throughout the day and weekends. I would also like to thank the University Honors Program for this unique milestone experienced by few undergraduate students and the constant support they have provided throughout the entirety of my studies. Most of all, I hold the most gratitude to my parents, Mark and Leigh, whose faith in me and encouragement never wavered even through bouts of tension and uncertainty.

INTRODUCTION

Thermal management systems are integrated into devices to ensure constraints, like various component temperatures, remain within the operational range of the device. Typically, the heat produced as a result of operation can hinder or even harm performance. Electronics typically require extended surfaces to remove this heat from the source. These surfaces function by increasing the surface area of the device, often in the form of fins projecting outward, to facilitate heat transfer to the ambient environment.

Heat created during operation is commonly referred to as "waste heat" because it offers no benefit and can hinder functionality. Removal proves necessary for industries like aerospace where it must be recycled as useful energy or dissipated to the surroundings. In an environment like outer space where thermal radiation is the only mode of heat transfer, typically, flat-plate radiators are attached to the surface of the aircraft to regulate the overall shuttle but similarly systems with individual temperature limitations relative to their neighboring components. Since aerospace flight is an immensely costly endeavor heavily dependent on weight constraints, it is crucial that its thermal management system add the least amount of mass to the spacecraft while maximizing heat transfer. Weight reduction is critical in similar fields where even the minimal addition of weight can grossly affect not only the overall weight of the assembly, but the weight in one area causing a rotational moment altering the center of gravity of the shuttle. This in turn could disrupt other systems and functions of the entire assembly. Even with less complex projects, considering weight and material reduction can prove to be a cost-effective asset during the design process.

Commented [SF1]: Inconsistent with spacecraft

Simple rectangular and triangular geometries embody conventional fin shapes; fractal patterns utilize these simplistic shapes as their zeroth iterations whilst building with complexity per each continued iteration. The geometries examined in the study are called fractal-like fins. Fractal geometries have been found in several studies to increase a fin's thermal performance. Both the reduction of volume and mass of the material used along with an increase in performance of the fin are desirable to prevent malfunction of the device or machine through passive heat dissipation. The pattern studied in this research is the Sierpinski carpet fractal pattern, seen in fig. 1, which begins with a fundamental solid square fin where an increasing number of perforations are incorporated through each iteration successively reducing the fin's mass while increasing its surface area simultaneously; this increase in surface area increases the rate of heat transfer experienced across the fin. For this project, it is desirable to find the most efficient rate of heat transfer across the fin, moreover, to reduce mass simultaneously, where possible. The reduction in mass results from the incorporation of perforations which removes material in each fin, and by extension, its respective weight.

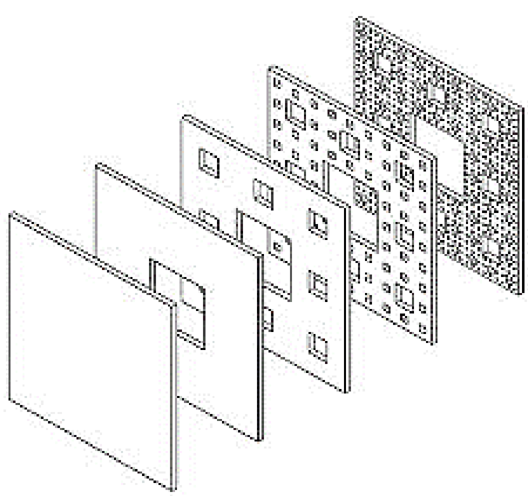

Figure 1: The Zeroth-Fourth Iterations of the Sierpinski carpet Fractal Pattern [1]

Background

Literature Review

This review was completed to familiarize myself with the foundations of various mechanisms of heat transfer to prepare me to begin research. Heat sinks used in electronics, specifically microelectronics, will be the focus of this research. Six papers were examined in this review all focusing on various shapes of fins beyond the typical rectangular and triangular geometries that aid in the dissipation of heat away from the device surface to which they are attached. These geometries are called fractal-like fins; the two primary conventional patterns begin from the zeroth iteration where material is either added or removed. The Sierpinski carpet fractal pattern begins with a fundamental square fin in which perforations are incorporated with each iteration successively reducing mass and increasing surface area simultaneously; this increase stimulates the rate of heat transfer experienced across the fin. The second fractal pattern, the Koch Snowflake, begins with an equilateral triangle as the zeroth iteration adding similar geometric extensions to the original with continued iteration thereby increasing surface area similar to its counterpart. Only the Sierpinski carpet was studied in this research; background discussing the Koch Snowflake is only given for detail and context.

"Natural Convection Heat Transfer from Fractal-Like Fins"

This study compares a basic square fin (the zeroth iteration) to the following four iterations of Sierpinski carpet fractal pattern. This was performed through natural convection alone and a constant heat flux applied at the base of each fin. Fin effectiveness was found to greatly increase because of the characteristics of increased surface area per volume of fractal patterns. Fin effectiveness, in relation to its reduced mass, was seen to greatly increase as well, improving with each iteration increasing at a minimum of 37% after the fourth iteration. Fin effectiveness per unit mass improved more significantly for thicker fins at about 303% for a width-to-thickness ratio of 8 after four iterations. An increase in heat flux of 800% only yielded a reduced fin effectiveness of 3.7%; therefore, the adverse effects caused by heat flux were negligible. With decreasing fin width, fin effectiveness increased; effectiveness improved 19% for a fin width of .01 m while a width of 1 m yielded a 7% decrease. The largest difference in effectiveness for orientation relative to gravity was 4%; therefore, the fins were determined to behave independently of orientation. [2]

"Average View Factors for Extended Surfaces with Fractal Perforations"

This study focused on average fin view factors as a function of fractal iteration and width-to-thickness ratio of the Sierpinski carpet pattern. As the iterations progressed, the respective surface area increased accordingly. Accordingly, the magnitude of intersurface thermal radiation within the perforations increased with each increasing iteration.

The fourth iteration had about 23.3% more surface area compared to a solid, rectangular fin of identical material and dimensions. The same fin only emits 67.36% of the radiation to its surroundings caused by intersurface radiation, which was found to be a function of the perforation level along with the width-to-thickness ratio of the extended surface. Increasing fin thickness resulted in a decrease in the thermal radiation emitted from the surface within the perforations. The average view factor approached zero after a finite number of iterations regardless of width-to-thickness ratio; therefore, there exists a finite limit at which iterations following may negatively impact thermal performance. [3]

"Natural Convection Fin Performance Using Fractal-Like Geometry"

The first three fractal iterations of the equilateral triangle and the square fin geometries of the Koch Snowflake and the Sierpinski carpet, respectively, with equal base lengths were compared in this study. As iterations progress, the Modified Koch Snowflake pattern adds material; conversely, the Sierpinski carpet pattern removes material. However, both methods increase the surface area of its zeroth model as the iterations advance.

Constant heating conditions were applied at the fins' bases read by an infrared camera. Fin effectiveness and efficiency were calculated for each iteration. The increase of heat transfer peaked after several iterations for each respective pattern, after which effectiveness generally decreases. The effectiveness of the first three iterations can be predicted by comparing the baseline case and the relative surface area. Fin effectiveness held a proportional relationship to surface area which was shown by an increase of 11.4% in the third Sierpinski iteration and up to 44.8% in the third Koch iteration. Effectiveness per mass increased dramatically in the third Sierpinski iteration by almost 60% while its counterpart only increased by 6%. [4]

"Mixed and Forced Convection Heat Transfer Characteristics of Sierpinski Carpet Fractal Fins"

This study assessed thermal performance under an incrementally increasing input power of 10, 20, and 30 Watts with uniform velocities of 1, 2, and 4 m/s in mixed and forced convection environments. Fin effectiveness behaved independently of power input but dependently on the magnitude of velocity applied. Fin efficiency decreased per iteration while fin effectiveness per unit mass increased regardless of power or velocity. At a uniform velocity of 1 m/s, the fourth iteration of the Sierpinski carpet fractal pattern was 6.67% more effective, 13.66% less efficient, and 71.01% more effective per unit mass

Commented [SF2]: Independently independently compared to its zeroth version. Alternatively, the fourth iteration was less effective at higher velocities regardless of power input. This signified that the Sierpinski Carpet patterns are more appropriately suited for low-velocity, passive heat transfer environments rather than when subjected to forced convection. [5]

“Experimental Effectiveness of Sierpinski carpet Fractal Fins in Natural Convection Environment”

Steady power inputs of 2.5, 5, 10, and 20 Watts were applied to fins made of Aluminum 5052-H32. Fin efficiency decreased as iterations progressed while fin effectiveness per unit mass increased. A design inspired by the fourth Sierpinski iteration was more effective than the traditional equilateral rectangular fin; the fourth iteration was also 3.63% more effective, 16.19% less efficient, and 65.99% more effective per unit mass. The total amount of heat transfer attributed to thermal radiation, on average 57% of the total at the baseline case, changed with each iteration: 53.67%, 50.33%, 48.84%, and 45.84% for the first four iterations, respectively. [6]

“Radiant Fin Performance Using Fractal-Like Geometries”

This study by Dannelley and Baker focuses on the comparison of two thermally radiating fractal-like fins, both the Sierpinski carpet and Koch Snowflake patterns. The first five iterations of each were examined. Each fin base was heated isothermally radiating to the ambient environment. Effectiveness per unit mass significantly improved up to 46%; however, this can be reduced for thicker fins. For the Sierpinski iterations, the fin effectiveness per unit mass was found to increase even while fin effectiveness decreased. For the same fractal patterns, aluminum was found to increase fin effectiveness by an order of two times that for copper. The Koch Snowflake did not perform as well as its counterpart where effectiveness per unit mass merely increased 1.6%. [7]

EXPERIMENTATION

The zeroth iteration of the Sierpinski carpet fractal pattern is a straight, square fin of uniform cross section. With each successive iteration, a rising quantity of square perforations of decreasing size are added, thereby decreasing its original mass while simultaneously increasing its surface area depending on the width-to-thickness ratio of the pattern. The experimental setup shown in fig. 2 details the fin's orientation in relation to the infrared camera; the camera always remained perpendicular to the fin's face including when altering fin orientation. A heating element read by a T-type thermocouple was adhered below the fin's base inside the melamine foam in which it is situated. This element was also connected to the DC power box that supplied a voltage of 20 Volts and an amperage of 1 ampere.

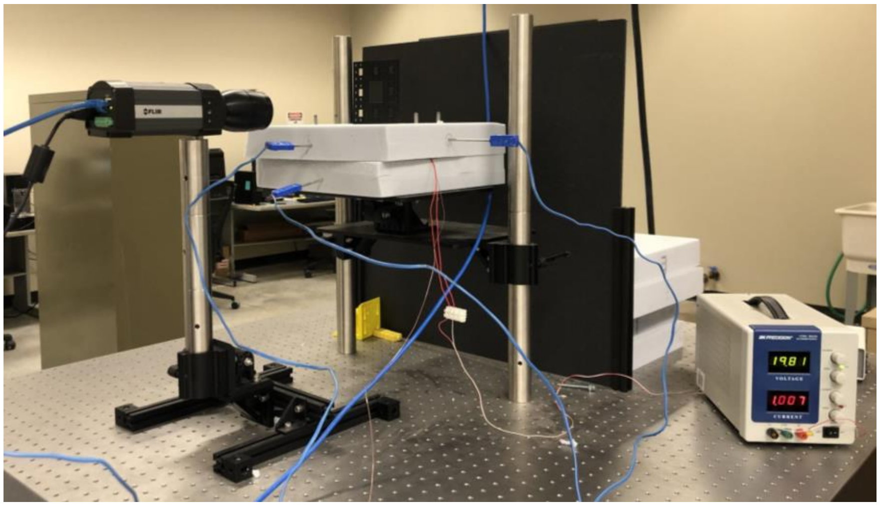

Figure 2: Experimental Setup at an Orientation of 90°

The TechLite Flexible Open-Cell melamine foam has a flashpoint temperature of 350°C (662°F); therefore, testing did not exceed this range. Four T-type thermocouples were inserted into the foam to measure the temperature of the area surrounding the fin: T_{tip}, T_{base}, and T_{amb}.. Their placement remained constant throughout all trials. A blackboard placed behind the experimental setup acted as a blackbody providing a background free of other potentially heat-producing entities that could be registered by the real-time thermal camera, the FLIR A325sc. Not shown, the camera was connected via USB to a computer to communicate with the FLIR ResearchIR software and LABView which was programmed to interpret the temperatures read by all thermocouples; an additional K-type thermocouple measured the ambient temperature of the room which varied from 21-24°C (69-75°F).

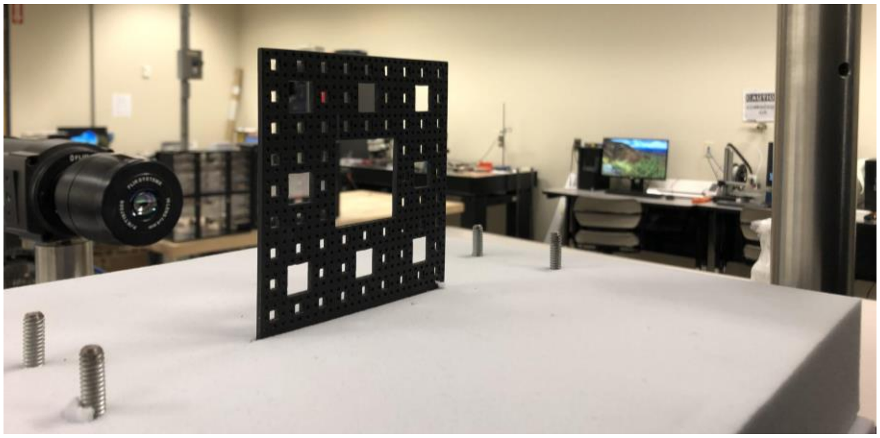

Figure 3: The Fourth Iteration of the Sierpinski carpet Fractal Pattern

This series of experiments was performed with natural convection acting as the sole mechanism for heat transfer with a constant heat flux of 20 Watts applied at the base of the fin. Each fin is an equilateral square with dimensions of 101.6 x 101.6 millimeters (4 x 4 in) and a uniform thickness of 3.175 mm (⅛ in). All fins are made of Aluminum 5052-H32.

Table 1: Surface Area and Mass of the Five Iterations of Fins

n	As (cm^2)	m (g)
0	212.90	87.83
1	194.26	78.08
2	185.34	69.40
3	197.80	61.69
4	263.25	54.83

Fins were heated starting at room temperature before every trial via the heating element strip attached below the base encased within the foam creating isothermal base temperatures throughout all trials. The camera remained at a constant distance from the fin which worked conjunction with the FLIR software to read base and tip temperatures. All five iterations were examined at the three orientations of 0°, 45°, and 90° for five trials each. All values were recorded when the temperature reached steady state. Heat flux applied was then halted and the fin left to cool to ambient temperature to prepare for the following trial.

DATA

Table 2: Constant used in Calculations

k_{ins}	0.036	W/m·K
k_{air}	0.02624	W/m·K
k_{alum}	138	W/m·K
ν	1.57E-05	m^2/s
Pr	0.713	
ε	0.99	
σ	5.67E-08	W/m^2K^4
g	9.81	m/s^2

Fin efficiency *η,* effectiveness *ε,* and effectiveness per unit mass ε_m were calculated for each trial of each iteration and then averaged. It was predicted that fin efficiency would decrease as the angle of orientation decreased up to the third iteration and that effectiveness may increase with increasing angle of orientation; however, the gathered data, seen in Tables 3-5, led to different conclusions.

CALCULATIONS

The targeted metrics to be calculated from collecting data such as temperature are efficiency η, effectiveness ε_{fin}, and effectiveness per unit mass $\varepsilon_{fin/m}$. Efficiency was one of three attributes of fin performance assessed in these experiments. This ratio compares the actual rate of heat transfer from the fin to the surrounding fluid, in this case ambient air, to the ideal rate of heat transfer; this ideal rate assumes that the entire surface of the fin is at base temperature. [8] Efficiency can be calculated according to the following equation,

$$\eta = \frac{Q_{conv}}{hA_s(T_b - T_{amb)}}$$

where Q_{conv} is the convective rate of heat transfer. This was found by subtracting the thermal radiation and the heat loss in the insulation from the 20 W of power supplied to the fin seen below:

$$Q_{conv} = P - Q_{loss} - Q_{rad}$$

These values give rise to the average heat transfer coefficient, h. [6]

$$h = \frac{Q_{conv}}{hA_s(T_s - T_{amb)}}$$

The effectiveness of the fin was investigated in this study to assess at what level the rate of heat transfer increased. It can be further defined as ε, the ratio between the heat transfer of the fin and the rate of heat transfer without the fin.

$$\varepsilon = \frac{Q_{conv}}{hA_b(T_b - T_{amb})}$$

Effectiveness per unit mass was the third metric calculated. Per unit mass can also be termed "mass-specific." Therefore, fin effectiveness per unit mass measures the effectiveness of a single kilogram of the fin. [9] This evaluation is necessary when mass reduction is critical. [7]

The following temperatures gathered were used in calculation. T_{amb}, T_{lat}, T_{long}, and T_{below} were gathered from the thermocouples within the foam. $T_{tip,max}$ and T_{tip}, min were averaged to find T_{tip}; likewise, $T_{base,max}$ and $T_{base,min}$ were used to find T_{base}. These values were measured by the infrared camera.

Table 3: Averages of Efficiency, Effectiveness, and Effectiveness per Unit Mass at 0°

	η			ε			ε/m_n (kg^{-1})		
n	Avg.	Std.	C.I. ±	Avg.	Std.	C.I. ±	Avg.	Std.	C.I. ±
0	0.88	0.003	0.003	58.09	0.18	0.23	661.32	2.10	2.61
1	0.87	0.015	0.018	52.61	0.89	1.10	673.82	11.34	14.08
2	0.83	0.008	0.010	47.68	0.48	0.60	687.06	6.97	8.65
3	0.78	0.006	0.007	47.56	0.35	0.44	770.97	5.74	7.12
4	0.76	0.006	0.007	61.79	0.35	0.44	1126.83	5.74	7.12

Table 4: Averages of Efficiency, Effectiveness, and Effectiveness per Unit Mass at 45°

	η			ε			ε/m_n (kg^{-1})		
n	Avg.	Std.	C.I. ±	Avg.	Std.	C.I. ±	Avg.	Std.	C.I. ±
0	0.88	0.017	0.021	58.25	1.13	1.41	663.13	12.92	16.04
1	0.85	0.005	0.006	51.49	0.31	0.39	659.47	4.00	4.96
2	0.82	0.010	0.013	47.25	0.59	0.74	680.76	8.55	10.62
3	0.78	0.011	0.014	47.58	0.68	0.84	771.24	10.99	13.65
4	0.72	0.011	0.014	58.77	0.68	0.84	1071.71	10.99	13.65

Table 5: Averages of Efficiency, Effectiveness, and Effectiveness per Unit Mass at 90°

	η			ε			ε/m_n (kg^{-1})		
n	Avg.	Std.	C.I. ±	Avg.	Std.	C.I. ±	Avg.	Std.	C.I. ±
0	0.89	0.003	0.004	58.92	0.23	0.28	670.83	2.61	3.24
1	0.87	0.004	0.004	52.18	0.21	0.26	668.28	2.71	3.37
2	0.84	0.009	0.011	48.54	0.50	0.62	699.44	7.18	8.92
3	0.82	0.015	0.019	50.44	0.93	1.16	817.59	15.12	18.77
4	0.78	0.015	0.019	63.34	0.93	1.16	1155.13	15.12	18.77

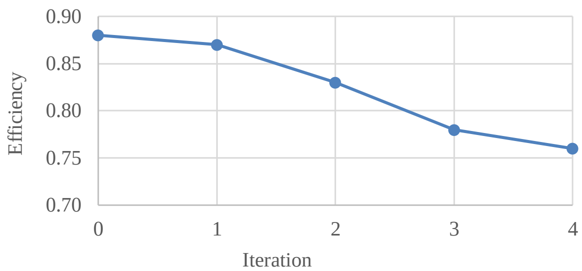

Figure 4: Average Efficiency at 0°

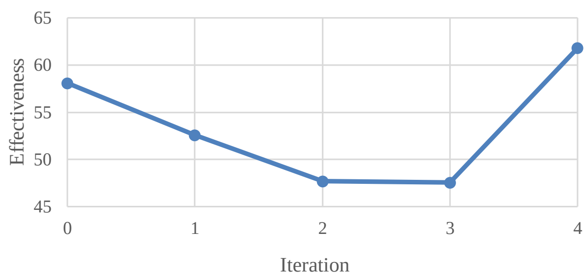

Figure 5: Average Effectiveness at 0°

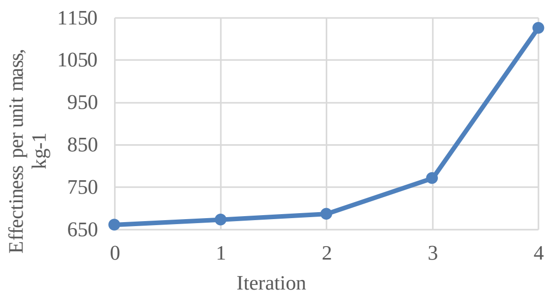

Figure 6: Average Effectiveness per Unit Mass at 0°

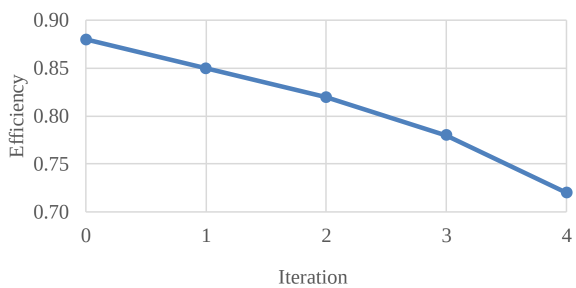

Figure 7: Average Efficiency at 45°

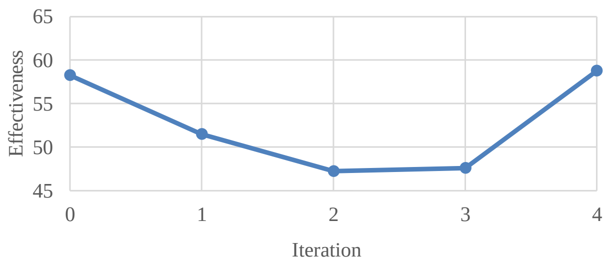

Figure 8: Average Effectiveness at 45°

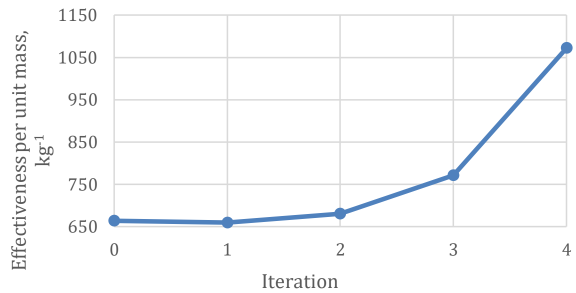

Figure 9: Average Effectiveness per Unit Mass at 45°

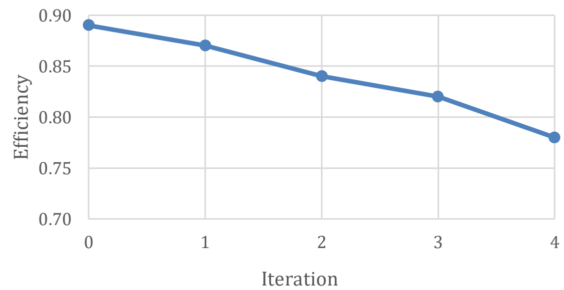

Figure 10: Average Efficiency at 90°

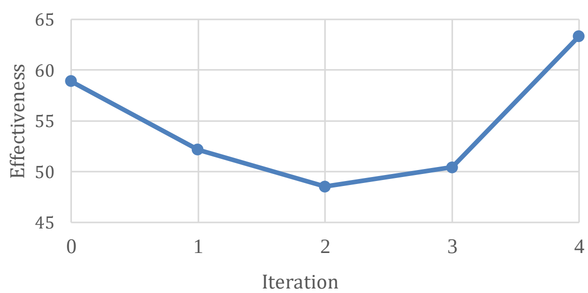

Figure 11: Average Effectiveness at 90°

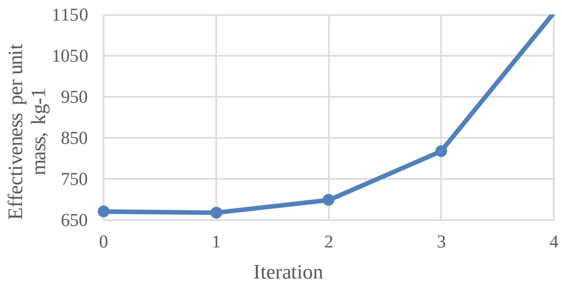

Figure 12: Average Effectiveness per Unit Mass at 90°

Referring to the graphs in figs. 3-12 using the data from Tables 3-5, more visual comparisons between iterations and orientations can be constructed. Generally, all three categories followed the same trends across all iterations and orientations. Efficiency across the board slowly decreased from about .9-.75. The orientation that provided the highest efficiencies was 90°. The 0^{th} fin was the most efficient iteration.

Effectiveness decreased from the 0^{th} - 1^{st} iteration reaching its lowest values of approximately 48 in the 2^{nd} and 3^{rd} iterations. ε_{fin} then began to rise again toward the 4^{th} iteration reaching its highest values from 59-64. Effectiveness was highest in the 4^{th} iteration at all angles but highest at an orientation of 90°.

Effectiveness per unit mass remained relatively consistent for the first two iterations beginning to increase exponentially around the 2^{nd} iteration to a maximum of approximately 1100 kg^{-1} in the 4^{th} iteration. This measurable occurred best at 90° in the 4^{th} iteration; however, the 4^{th} iteration held the highest values for $\varepsilon_{fin/m}$ throughout.

The plain fin performed with the greatest efficiency while the fourth iteration was most effective and most effective per unit mass. The greatest values for efficiency, effectiveness, and effectiveness per unit mass occurred at 90°. At 0° in the first iteration, effectiveness and effectiveness per unit mass were the only two values to be higher than any of their respective 90° values. All 90° values for all iterations were higher than those measured at 45°. At 0°, the 1st, 2nd and 4th iterations were all higher than their 45° counterparts for all three measurables. The third iteration ranked higher in efficiency alone. Therefore, at 45°, the 1st, 2nd, and 4th iterations performed the worst across all categories and orientations.

CONCLUSIONS AND RECOMMENDATIONS

Recommendations are intended for passive heat transfer only. Orientation of the fins was investigated to determine at what angle or range of angles would heat transfer be most efficient and effective. Because fins are added to the surface of devices or machinery, their orientation can vary based on their placement on the assembly; fins located on the side of a machine may perform differently from those placed on the top or those on an incline. These experiments offer insight on how fin orientation affects the heat transfer capabilities of the identical fins in different locations on the same assembly.

Based on the results, I would recommend avoiding placing any extended surfaces on inclines between 15-75°. Fins should be primarily focused on horizontal surfaces of the assembly, preferably top surfaces since heat will rise through the fins; at these locations they will behave in the most effective and efficient manner. Secondarily, if extended surfaces are not able to be installed around the 90° orientation, then they should be installed close to the 0° orientation as much as possible; positioned anywhere else on the assembly will yield lower levels of efficiency and effectiveness and may negatively impact the overall heat management system due to the excess weight. The weight added by the most efficient and effective fins is justifiable due to their performance, but any more additions will be considered excessive.

The preference of iteration to be implemented depends on the desired performance of the device. If a more efficient output is desired, earlier iterations should be used particularly the zeroth. The 2nd and 3rd iterations should be avoided at any angle when effectiveness is to be maximized. The 4th iteration yields the greatest effectiveness per unit mass in any orientation. However, efficiency will be sacrificed if an iteration with a higher effectiveness is implemented since they hold an inverse relationship.

These considerations were made based on data gathered from experiments with a constant power input of 20 W. A lesser or greater heat flux applied may alter the behavior of the heat transfer through the fins. Varying inputs of power or velocity would alter results since these trials occurred under free convection conditions.

NOMENCLATURE

A_b	Surface area of fin base, m^2
A_i	Surface area of fin embedded in insulation, m^2
A_s	Exposed surface area of fin, m^2
F_n	Average fin view factor
h	Average heat transfer coefficient, $W/m^2 \cdot K$
I	Current supplied, A
k	Thermal conductivity, $W/m \cdot K$
m	Mass, kg
n	Fractal iteration
P	Power supplied, W
$\dot{Q}_{conv}$	Heat dissipated by convection, W
$\dot{Q}_{loss}$	Heat loss through insulation, W
$\dot{Q}_{rad}$	Heat dissipated by thermal radiation, W
t	Thickness of fin, m
T	Temperature, °C
T_{amb}	Ambient temperature, °C
T_{base}	Average temperature at base of fin as measured by infrared camera, °C
T_s	Average surface temperature of fin (average of T_{base} and T_{tip}), °C
T_{tip}	Average temperature at tip of fin as measured by infrared camera, °C
V	Voltage supplied, V
w	Width of fin, m
w_s	Experimental uncertainty

ε	Emissivity
ε_{fin}	Fin effectiveness
$\varepsilon_{fin/m}$	Fin effectiveness per unit mass, kg^{-1}
η	Fin efficiency
ρ	Density, kg/m^3
σ	Stefan-Boltzmann constant, 5.67×10^{-8} $W \cdot m^{-2} \cdot K^{-4}$

REFERENCES

[1] Shaffer, Jennifer P., "Investigation of the Thermal Performance of Sierpinski carpet Fractal Fins in a Natural Convection Environment" (2017). University Honors Program Theses. 265.

[2] Dannelley, Daniel. John Baker. *Natural Convection Heat Transfer from Fractal-Like Fins.* Journal of Thermodynamics and Heat Transfer. July 2013.

[3] Calamas, David, Daniel Dannelley. *Average View Factors for Extended Surfaces with Fractal Perforations.* Case Studies in Thermal Engineering 12 (2018) 701-710.

[4] Dannelley, Daniel, John Baker. *Natural Convection Fin Performance Using Fractal-Like Geometries.* Journal of Thermodynamics and Heat Transfer Vol. 26 No. 4, October-December 2012.

[5] Calamas, David. Tiesha Wolfe. Valentin Soloiu. *Mixed and Forced Convection Heat Transfer Characteristics of Sierpinski carpet Fractal Fins.* Heat Transfer Research 50 (3): 263-285 (2019).

[6] Calamas, David. Daniel Dannelley. Gyunay H. Keten. *Experimental Effectiveness of Sierpinski carpet Fractal Fins in Natural Convection Environment.* Journal of Heat Transfer, Vol. 139. September 2017.

[7] Dannelley, Daniel. John Baker. *Radiant Fin Performance Using Fractal-Like Geometries.* Journal of Heat Transfer, Vol. 135. August 2013.

[8] Liu, Shenghui, Yanping Huang, Junfeng Wang. *Theoretical and Numerical Investigation on The Fin Effectiveness and The Fin Efficiency of Printed Circuit*

Heat Exchanger with Straight Channels. International Journal of Thermal Sciences. 21 June 2018.

[9] Micheli, Leonardo, K.S. Reddy, Tapas K. Mallick. *Thermal Effectiveness and Mass Usage of Horizontal Micro-Fins Under Natural Convection.* Applied Thermal Engineering 97 (2016) 39–47.